

Fluorescence-line-narrowing and energy-transfer studies in ruby

P. M. Selzer,* D. L. Huber, B. B. Barnett,[†] and W. M. Yen

Department of Physics, University of Wisconsin, Madison, Wisconsin 53706

(Received 29 August 1977)

Fluorescence-line-narrowing and time-resolved studies have been conducted in ruby crystals and powders, in concentrations varying from 0.025 to 0.9 at. %. The resonance fluorescence component of the R_1 line at low temperatures is observed to increase dramatically as the laser is tuned from line center toward the low-energy wing of the inhomogeneously broadened absorption. This is presumed to indicate the presence of weakly coupled pairs in the wings of the line. Intraline and interline ($R_1 \rightarrow N_{1,2}$) energy transfer have also been studied, and an elaboration of earlier work is given. Time-resolved selective-excitation scans have revealed numerous channels in the vicinity of the R lines by which the different pairs can be directly excited. These are assumed to be Cr ions near enough to a pair to be in a highly perturbed environment. Various experimental results are shown to be consistent with a model of rapid transfer between resonant Cr ions which feeds the pairs via a weak, nonresonant coupling to these perturbed ions. Macroscopic strain broadening is also shown to be favored over microscopic broadening, and the implications for Anderson localization in ruby are discussed.

I. INTRODUCTION

In many areas of experimentation there often evolves a standard—the one system presumed to be nearly “ideal” on which the most measurements have been made, the most is known, and hence the one on which new techniques are tried. For investigating the optical properties of impurity-doped ionic crystals, such a system is ruby ($\text{Al}_2\text{O}_3:\text{Cr}^{3+}$). The spectral lines of ruby were first reported long before the development of quantum-mechanical theory,¹ and the well-known sharp R lines were so labeled nearly 70 years ago.²

Since the development of the laser, the study of ruby has required both technological as well as purely scientific significance, and a large experimental and theoretical effort has been devoted to an understanding of the spectral details. Most of the static features of the spectrum, including lines originating from phonon sidebands and exchange-coupled pairs, are well understood,³ and the dynamics of nonradiative relaxation⁴ and also of energy transfer between isolated Cr ions and pairs⁵ have been extensively studied. Results of these latter experiments have led to the suggestion of ruby as a candidate for so-called “Anderson localization.”⁶

High-resolution tunable lasers, both pulsed and cw, have provided yet new spectroscopic techniques which when applied to ruby have revealed still new complexities. Photon echoes,⁷ fluorescence-line-narrowing,⁸ and hole-burning⁹ experiments have been devoted to the study of homogeneous line-broadening mechanisms of the R lines in the low-concentration low-temperature limit. Other related work¹⁰ has hypothesized the existence of mobility edges at higher concentrations

(0.09–0.23 at. %), taken as evidence for Anderson localization.

In two recent articles, Selzer, Hamilton, and Yen¹¹ and Selzer and Yen¹² have reported the results of time-resolved fluorescence-line-narrowing measurements spanning a large concentration range (0.025–0.9 at. %) and revealing some interesting spectral dynamics within the R_1 line. In fact, four distinct types of energy transfer have been postulated. In this article, spectral linewidth measurements are presented in addition to new and more detailed information about energy transfer. A model is proposed which appears to reconcile the seemingly contradictory experimental results on energy transfer obtained by different groups over the last decade.

II. EXPERIMENTAL DETAILS

The techniques used in these experiments have been discussed extensively in earlier publications,^{11,13} and only a few additional details need be provided here. Because the ground state in ruby is a doublet separated by 0.38 cm^{-1} , high-resolution studies with a Fabry-Perot interferometer may give ambiguous results if the etalon free spectral range is the same size or smaller than the doublet separation. This difficulty was circumvented with the use of two tandem etalons, one with a small spacer (1 mm) and one with a large spacer (8 mm). In this configuration, the resolution is determined by the large spacer, but the free spectral range (5 cm^{-1}) is set by the small one, resulting in an effective finesse of approximately 250 as compared to the single etalon value of ~ 30 .

The etalons were manually tuned for maximum

throughput near the frequency of interest and then pressure scanned across the fluorescence line, thereby maintaining their relative alignment. With careful adjustment, the parasitic modes of the 8-mm etalon had a transmission approximately 2% that of the central peak. With this arrangement, contributions to the narrowed linewidth 50–100 MHz greater than the instrumental profile could be resolved while scanning across the entire inhomogeneous profile (approximately 1 cm^{-1}).

An SSR 1120 amplifier-discriminator and a PAR 1110 counter were used for gated photon-counting measurements in conjunction with an RCA 31034A photomultiplier tube. The peak fluorescence signals were relatively large, with typically 1000 counts collected in 100 laser shots within a 20- μsec gate. Neutral density filters were used to reduce the fluorescence at early times, and longer counting periods used at large delays in order to maintain the peaks at roughly the same count level.

Low-resolution lifetime measurements were made using a 1-m spectrometer with an RCA 7265 tube, the output of which fed directly into either a boxcar integrator (PAR 162) or a signal averager (Nuclear Data Enhancetron 1024). The fluorescence profiles and lifetime data were normalized to the laser intensity before being plotted on a chart recorder.

Most of the samples examined in these experiments were flame fusion crystals obtained from Adolf Meller Co. They were carefully heat sunk to the cold finger of a variable-temperature cryostat or, for the 2-K range, placed in an immersion dewar. With measurements on ruby powders, an end-on geometry was used, and a mechanical chopper wheel, synchronized to the laser, interrupted the beam for approximately 1 msec during the excitation period.

III. LINEWIDTH STUDIES

It is well known that the R_1 line of ruby exhibits inhomogeneous (strain) broadening at low temperatures which is many orders of magnitude larger than the homogeneous linewidth. Using a hole-burning technique,⁹ Szabo has measured homogeneous widths in low-concentration ruby at 4 K to be roughly 10^{-3} cm^{-1} , whereas the inhomogeneous width is on the order of 1 cm^{-1} . Figure 1 shows excitation scans which reveal the inhomogeneous linewidths of two different concentration samples. In this procedure, the laser is tuned across the R_1 absorption line while the fluorescence is monitored with low resolution ($\sim 10 \text{ \AA}$) in order to encompass the entire line. The lower-concentration sample has the ground-state splitting still resolvable, whereas at higher concentration, the larger strain broadening completely masks this splitting.

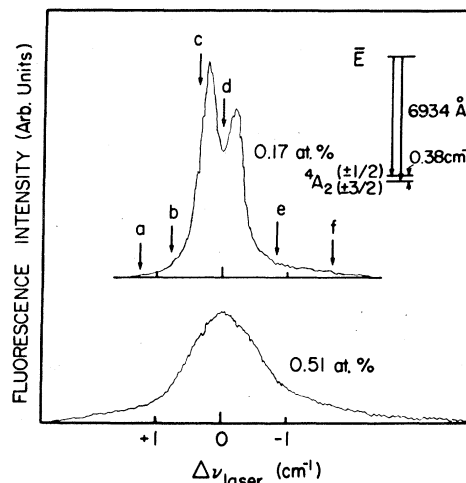


FIG. 1. Selective excitation scans of the R_1 line in ruby at 10 K for two different concentrations. The R_1 fluorescence is monitored with low (1-nm) resolution while the laser (~ 0.9 -GHz linewidth) is scanned across the absorption. The letters on the 0.17-at.% trace refer to fluorescence measurements shown in Fig. 3. The relevant energy levels of ruby are indicated in the upper right-hand corner.

Note in particular the rather long wings in these plots, especially on the low-energy side of the line. This phenomenon is discussed below.

A simple phenomenological model used to picture inhomogeneous broadening and fluorescence line narrowing (FLN) has been discussed in Ref. 12. Using this picture, one predicts that with the laser exciting either the high- or low-energy sides of the absorption line, there is only one set of ion sites with which the laser can interact. Hence, only two fluorescence lines will be seen, arising from the decay of the selected set of sites to both ground states. However, with the laser excitation near the middle of the line, two different sets of sites can simultaneously absorb (one set from each ground-state level) and consequently three fluorescence lines will be expected. This is exactly the type of behavior observed in concentrations up to approximately 0.4 at.%. At higher concentrations, which have considerable strain broadening and large wings, three lines are always observed.

Extending this model a bit further, it becomes possible to explain other features of the FLN spectra. In order to account for the wings of the line as shown in Fig. 1, we may draw the \bar{E} level with a discontinuous slope separating "normal" R_1 ions from the "abnormal" R_1 ions in the wings, as shown in Fig. 2. While this distinction is not strictly necessary as the slopes are completely arbitrary, this model allows us to distinguish more easily different types of ions, with one set

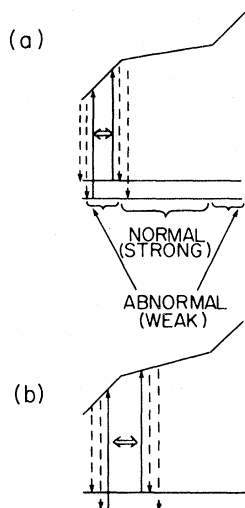


FIG. 2. (a) Laser excitation in low-energy wing of line where three fluorescence lines are expected. (b) Laser excitation on low-energy side of "normal" distribution. Since fluorescence from the "abnormal" ions is considerably weaker, only two strong fluorescence lines are expected.

presumably more strongly influenced by strains than another. The rationale for this distinction is discussed below.

With the larger slope for the abnormal ions, pumping far into the wing with the laser would again produce three lines since the laser can once again interact with two different (abnormal) sites. When pumping at the edge of the normal-ion absorption, the laser interacts with one normal site and one abnormal site, but because emission from the latter is considerably weaker than the former, only two predominant lines will be seen. The two different cases are shown schematically in Figs. 2(a) and 2(b), respectively.

These various predictions have all been experimentally verified for a 0.17-at. % sample at 10 K, and exemplary traces are shown in Fig. 3. Note also that as the laser probes farther into the wings, the lines appear to broaden. In order to investigate this phenomenon, a series of moderately-high-resolution linewidth measurements have been made as a function of laser excitation frequency within the R_1 line for crystals of different concentrations and at different temperatures.

When an absorption line is probed with a high-resolution laser and the width of the resonance fluorescence subsequently measured, it has been shown that in the absence of spectral dynamics, the experimental linewidth is then¹⁴

$$\Delta\nu_{\text{exp}} = \Delta\nu_{\text{ins}} + 2\Delta\nu_{\text{homo}}, \quad (1)$$

where $\Delta\nu_{\text{ins}}$ is the instrumental linewidth (convol-

uted laser and interferometer profiles) and $\Delta\nu_{\text{homo}}$ is the homogeneous width, or at least a residual width not associated with static strains.

If spectral dynamics which broaden or in other ways alter the fluorescence lineshape are occurring, the homogeneous width may still be extracted by making a gated measurement at sufficiently short delays after the laser pulse. This, of course, assumes that the dynamics occur on a time scale longer than the instrumental response time. Since even at relatively high concentrations the spectral dynamics in ruby are quite slow at low temperatures,¹¹ gated measurements with a gate width of 10 μsec and a delay of $\leq 5 \mu\text{sec}$ after the pulse were sufficient to adequately isolate the narrowed component.

In Fig. 4 a plot of linewidth of the fluorescence component in resonance with the laser-versus-laser position is shown for different Cr concentrations at 10 K. Note the rather abrupt increase with the laser probing the low-energy wing of the line. The

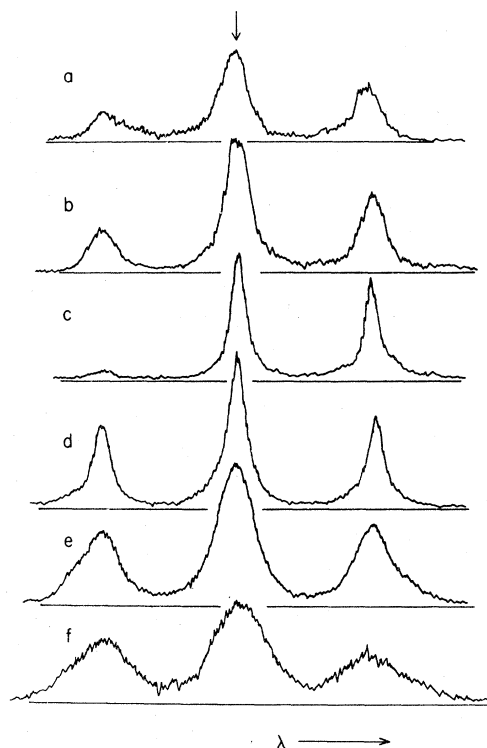


FIG. 3. Representative fluorescence scans at "zero" delay (typically 10- μsec delay with a 20- μsec gatewidth) for a 0.17-at. % sample at 10 K. The letters refer to the different laser pump frequencies indicated in Fig. 1. In each case, the peaks are separated by the ground-state splitting of 0.38 cm^{-1} . The instrumental linewidth is reflected in traces *c* and *d*. Arrow points to the resonance fluorescence component.

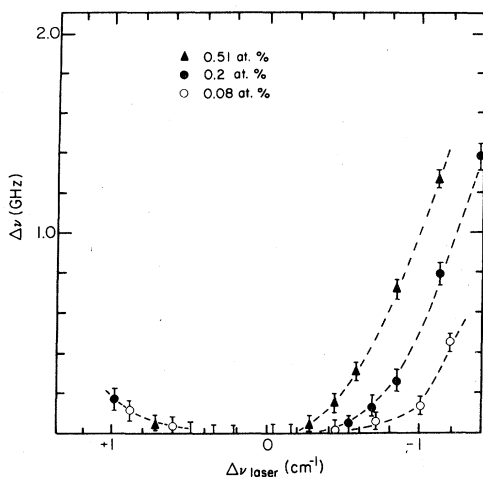


FIG. 4. Linewidth of the resonance fluorescence component vs laser pump frequency for different concentration samples at 10 K.

onset of this increase corresponds roughly to the position of the anomalous wings in the excitation scans. Furthermore, these linewidths show no detectible increase with temperature between 2 and 40 K.

If the large widths are homogenous, arising from an increased ion-lattice coupling for these abnormal ions, than a strong temperature dependence would be expected because of the inferred phonon-induced relaxations.¹⁵ We therefore propose that these are not homogeneous lines but rather reflect an unresolved splitting of both the excited and ground-state levels of these ions, which manifests itself in fluorescence (to the split ground state), and which increases the farther one probes from line center. With an instrumental width of approximately 1.8 GHz, lines split by less than 1 GHz would be totally unresolved, and since the individual components are still assumed to be approximately as narrow as the measured homogenous widths,⁹ no increase in the observed linewidth would be expected until the homogeneous width of the components broaden significantly with temperature (which starts at ~40–50 K).

This picture would suggest that the abnormal ions are really very weakly coupled pairs or clusters of ions. Their mutual interaction slightly shifts and lifts the degeneracy of the energy levels, but to a much lesser extent than the discrete well-known exchange-coupled pairs.³ The presence of weak clusters underlying the R_1 absorption seems very plausible, and has been proposed as an explanation for anomalous photon-echo results in the low-energy wing of R_1 .¹⁶ Our results appear to corroborate this interpretation.

IV. ENERGY TRANSFER

We turn now to the details of the different energy-transfer mechanisms in ruby, both within the R_1 line and between the R lines and N lines (pairs).

A. Intraline nonradiative transfer

In concentrations of ≥ 0.08 -at. % Cr, it has been found that after narrow-band laser excitation, the initially excited ions feed energy via a phonon-assisted process into the full inhomogeneous background.¹¹ From the temperature and concentration dependence of this process, and also from measurements on powders (in order to reduce any radiative trapping), a nonradiative one-phonon-assisted process has been deduced.

Typical scans for a 0.9-at. % sample are shown in Fig. 5, where the distinction between background and narrowed components is quite apparent. For the large inhomogeneous broadening of this sample, three narrowed components are observed (see Sec. III). In all cases, as mentioned in Refs. 11 and 12, there are some photons detected even at zero delay at the position of the background (refer to the $t=0$ trace of Fig. 5). This might be due in part to the long wings of the near-Lorentzian instrument profile or to direct excitation of the background through phonon-assisted absorption. However, when the transfer rate is of the same order or faster than the radiative decay of the line, an absolute rise of the background is always detected—in this case, the maximum being nearly twice the $t=0$ value. It should be emphasized that

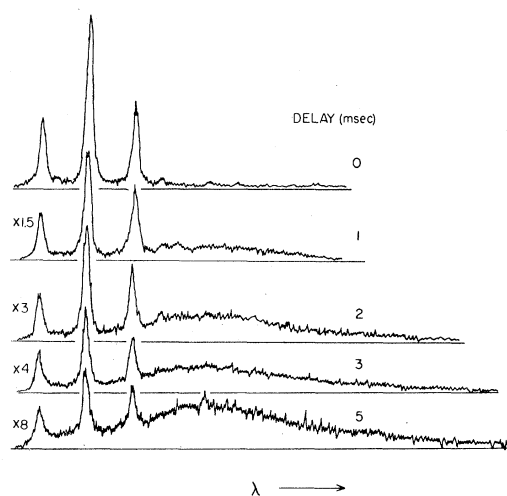


FIG. 5. Time delay study for a 0.9-at. % sample at 10 K. The laser excitation is somewhat on the high-energy side of line center. The narrowed peaks are separated by 0.38 cm^{-1} . Gain settings relative to the zero-delay trace are shown on the left-hand side.

any rise of the background whatsoever is sufficient to prove that the process involves a flux of energy and not merely a slower decay of the broad component of the line. Furthermore, if we assume that in the absence of energy transfer, the initially excited broad background decays at the same rate as the narrowed components, then its presence does not invalidate our data analysis: it merely becomes part of the narrowed-component line-shape which is used to fit the subsequent data at later delays. The above assumption seems very plausible, as no significant variations in radiative decay are observed across the inhomogeneous absorption, and under intentional broadband excitation, the lifetime is the same as with the usual narrow-band source.

The temperature and concentration dependence of the transfer rate are given in Fig. 2 of Ref. 11, where the characteristic transfer time is defined as the $1/e$ point in the ratio of the narrowed to the total intensity plotted as a function of time, and the rate defined as the inverse of this time. Alternative methods of extracting a transfer rate are discussed in Sec. IV B.

One-phonon-assisted or "direct" energy transfer has been proposed by Orbach¹⁷ and later elaborated on by Birgeneau.¹⁸ Using the Golden Rule approach with third-order perturbation theory, the transfer rate of electronic excitation from ion 1 to ion 2 involving the emission or absorption of a single phonon of energy $\hbar\omega_p$ may be written

$$W_{\text{dir}} \approx \frac{2\pi}{\hbar^2} J_{1,2}^2 \frac{\omega_p}{4\pi^2 \hbar \rho v^3} |\Delta M^{(1)} - \Delta M^{(2)}|^2 (n_{\bar{k}} + \gamma), \quad (2)$$

where $J_{1,2}$ is an average ion-ion coupling (exchange or multipolar), ρ is the mass density, v is the appropriately averaged sound velocity, and γ is 1 (0) for phonon emission (absorption). The temperature dependence arises from the Bose occupation term $n_{\bar{k}} = [\exp(\hbar\omega_p/kT) - 1]^{-1}$, and $\Delta M^{(i)}$ is the difference in ion-lattice coupling strength between the excited and the ground state for the i th ion. For the concentrations and phonon wavelengths involved we assume the long-wavelength approximation to be valid, so the phase factor has been taken as unity. Note that if the strain coupling at site 1 is nearly equivalent to that at site 2 then the difference between ΔM 's is likely to be but a few percent of either $\Delta M^{(1)}$ or $\Delta M^{(2)}$.

At all the temperatures accessible to us, $kT \gg \hbar\omega_p$ and, generally, $kT \gg \hbar\omega_p$. The Bose factor can then be simplified to $n_{\bar{k}} \approx kT/\hbar\omega_p$, in which case the ω_p 's cancel, and we are left with an expression for the direct process which is explicitly independent of the energy mismatch (although an implicit dependence may still exist due to variations of J or ΔM across the absorption line) and linear

in temperature. This is exactly the behavior observed for all samples between 0.08 and 0.9 at. % in the range 5–50 K (refer to Fig. 2, Ref. 11), and for laser excitation within the "normal" portion of the line. Far into the wings, different rates are observed, as discussed below. Above 60 K other phonon-assisted processes probably become effective.

The direct process is not the only possible non-resonant energy-transfer mechanism. A higher-order phonon-assisted process, exhibiting T^3 behavior, has been recently observed in $\text{LaF}_3:\text{Pr}^{3+}$ and PrF_3 ,^{19,20} and various higher-order processes have been examined theoretically by Holstein, Lyo, and Orbach.²¹ Particularly relevant to ruby is the two-phonon "resonant" process, W_{res} of Ref. 21. In this case, the excitation transfer is accompanied by a phonon-induced transition from the \bar{E} level to the $2\bar{A}$ level (29 cm^{-1} above) and back down. The difference in energy between the absorbed and emitted phonons conserves total energy for this process.

The transition probability for the resonant process may be written²¹

$$W_{\text{res}} = \left(J_{\bar{E}}^2 + \frac{(\Delta E_{1,2})^2 J_{2\bar{A}}^2}{(\Delta E_{1,2})^2 + \Gamma(2\bar{A})^2} \right) \times \frac{1 + \exp(-\Delta E_{1,2}/kT)}{(\Delta E_{1,2})^2} W_{\bar{E} \rightarrow 2\bar{A}}, \quad (3)$$

where once again, J is an average ion-ion coupling, only here $J_{\bar{E}}$ refers to the excited ion in the \bar{E} state and $J_{2\bar{A}}$, in the $2\bar{A}$ state. $\Delta E_{1,2}$ is the energy mismatch between sites 1 and 2, $\Gamma(2\bar{A})$ is the phonon-induced width of the $2\bar{A}$ level, and $W_{\bar{E} \rightarrow 2\bar{A}}$ is the non-spin-flip transition rate between the \bar{E} and $2\bar{A}$ levels. Since kT is generally much larger than $\Delta E_{1,2}$, the second term in parentheses is approximately $2(\Delta E_{1,2})^{-2}$, and the dominant temperature dependence arises from the $W_{\bar{E} \rightarrow 2\bar{A}}$ term. Also, $\Delta E_{1,2}$, which can be taken as approximately the inhomogeneous width, is considerably larger than $\Gamma(2\bar{A})$. Thus, with the further assumption that $J_{\bar{E}} \approx J_{2\bar{A}}$, Eq. (3) can be simplified to

$$W_{\text{res}} \approx [4J^2/(\Delta E_{1,2})^2] W_{\bar{E} \rightarrow 2\bar{A}}. \quad (4)$$

By using the general expression for phonon-induced relaxation,²²

$$W = (3\omega^3/2\pi\rho v^5\hbar) |M|^2 n_{\bar{k}}, \quad (5)$$

where the symbols are the same as in Eq. (2), and plugging this into (4) for $W_{\bar{E} \rightarrow 2\bar{A}}$, it is then possible to estimate which processes should dominate the low-temperature range. Using (2), (4), and (5) we arrive at the expression

$$\frac{W_{\text{res}}}{W_{\text{dir}}} \cong 12 \left(\frac{\omega_{\bar{E}, 2\bar{A}}}{\omega_{1,2}} \right)^3 \left(\frac{M_{\bar{E}, 2\bar{A}}}{\Delta M^{(1)} - \Delta M^{(2)}} \right)^2 \times \exp \left(\frac{-42}{T} \right) \frac{\hbar\omega_{1,2}}{kT}. \quad (6)$$

Here $\omega_{\bar{E}, 2\bar{A}}$ refers to the 29-cm⁻¹ phonons active in the resonant process, whereas $\omega_{1,2}$ refers to the roughly 1-cm⁻¹ phonons of the direct process. Also, $M_{\bar{E}, 2\bar{A}}$ is the off-diagonal strain-matrix element between the \bar{E} and $2\bar{A}$ levels, whereas the ΔM 's in the denominator refer to the difference in diagonal strain elements between the \bar{E} level and the ground state (⁴A₂). In this approximation, the crystal is assumed to be isotropic, and the temperature range of interest is taken to be $1 < kT < 29$ cm⁻¹. With the final assumption that $M_{\bar{E}, 2\bar{A}} \sim \Delta M^{(1)} - \Delta M^{(2)}$ and they therefore cancel (the validity of which will be discussed below), we then find from Eq. (6) that (contrary to the experimental results) W_{res} should dominate above approximately 5 K and exceed W_{dir} by nearly three orders of magnitude in the 10–20 K range.

This discrepancy between theory and experiment requires some consideration. A number of approximations have been made in the derivations of Eqs. (2) and (3) and, additionally, in obtaining quantitative estimates for Eq. (6). Probably the largest unknown arises from the strain-matrix elements. $M_{\bar{E}, 2\bar{A}}$ has been calculated by Blume *et al.*²³ to be approximately 1600 cm⁻¹, but recent lifetime measurements of the R_2 line²⁴ show this value to be too large by almost a factor of 2.

On the other hand, $\Delta M_{\bar{E}, 4A_2}$ is only very roughly known. Using Schawlow's static strain data²⁵ and the elastic constants of ruby,²⁶ a value on the order of 3000–6000 cm⁻¹ is obtained. Furthermore, the degree of cancellation between $\Delta M^{(1)}$ and $\Delta M^{(2)}$ is even more uncertain. If ions 1 and 2 are in identical environments, then a large cancellation is expected, reducing the likelihood of the one-phonon process. However, the presence of abnormal ions or weak clusters folded into the R line, as proposed in Sec. III, may alter the picture.

It is well known that pair lines exhibit ion-lattice couplings which are considerably stronger than those of the single ions and which are also highly anisotropic.²⁷ It should also be noted from Ref. 27 that the maximum shift of a particular pair line for a given stress value of 100 kg/mm² (or piezospectroscopic sensitivity) is roughly equal to the value J of the exchange interaction for that pair. It seems reasonable to assume that more-distant pairs would scale in a similar fashion, and hence, the piezospectroscopic sensitivity (PS) for a weak pair (within the inhomogeneous R line) should also be on the order of J for that pair (which is approxi-

mately its position relative to line center).²⁸ Therefore, the PS of a pair within the inhomogeneous R_1 absorption can be of the same order as that for the isolated Cr ions (~ 1.5 cm⁻¹ for 100 kg/mm²).²⁵ Since the PS can be used to derive an approximate value for the ion-lattice coupling strength, we conclude that the ion-lattice coupling of even weak pairs can equal or exceed that of the single ions. In this case, because of the different symmetries and environments of the pairs and single ions, a large cancellation of strain-matrix elements would no longer be expected in the direct process. For example, if the ΔM in the denominator of Eq. (6) is only twice the larger of the values obtained from static strains, the squared ratio is $< 10^{-2}$, and the direct process is now of the same order as W_{res} in the temperature range of interest.

Clearly, the above discussion is merely a plausibility argument relating to the apparent dominance of the one-phonon process. It should not be considered as a resolution of the discrepancy between theory and experiment without more detailed information about the strain-matrix elements in this material.

Experimental evidence for the role of weak clusters in the energy-transfer process has been obtained in higher-concentration samples by monitoring the transfer rate when exciting far into the wings, particularly on the low-energy side where the anomalously large linewidths were measured. With the laser excitation 2 cm⁻¹ below line center, the transfer rate for the 0.9-at. % sample was more than five times faster than when pumping near the center; equidistant of the high-energy side, the rate was only twice as fast. This increased rate is considerably larger than would be expected from the small changes in n_{\pm} as a function of ω_{\pm} in Eq. (2), and most likely arises from an increase in the ion-lattice coupling for these abnormal ions.

It should be noted that the background shape remains constant within experimental error as a function of both time delay and excitation frequency, showing no tendency toward a greater weighting for the abnormal ions. However, any predictions for the spectral evolution of the line after narrow-band excitation must take into consideration both spectral and spatial distribution of the ions.²⁹ As discussed in Sec. IV E, the assumption of total microscopic randomness in ruby may be unfounded, making such predictions considerably more difficult.

We must also scrutinize the assumptions employed in the derivations of both Eqs. (2) and (3). While these equations have been derived assuming single-ion to single-ion transfer, evidence exists for a different model, as discussed in Sec. V: pho-

non-assisted energy transfer between groups of resonant ions, with a rapid, perhaps coherent, transfer within the group. A proper derivation for the phonon-assisted process would then involve sums over these groups of ions, and interference effects may prove significant. Also, since the excitation is presumably quite mobile within a given region, it can be pictured as moving from the initially excited site to one more favorable for transfer. While these effects are not likely to alter fundamentally the nature of phonon-assisted energy transfer, they may affect the approximations leading to Eq. (6) and, combined with the uncertainties in strain parameters, may fortuitously favor the one-phonon over the two-phonon process.

B. Time development of the nonradiative spectral transfer

In this section, we analyze the time dependence of the spectral transfer within the R_1 line. In making the analysis, we adopt a localized-state point of view. That is, we interpret the transfer as occurring between distinct sites on the corundum lattice. Reconciliation of the localized-state picture with the extended- or delocalized-state model introduced in the interpretation of the single-ion to pair transfer will be discussed in Sec. V.

In systems like ruby where the spectral transfer leads to background fluorescence which has the profile of the inhomogeneous line, the most appropriate quantitative measure of the transfer is the ratio of the intensity in the narrow line to the total intensity of the fluorescence in the inhomogeneous bandwidth. Formally, this ratio $R(t)$ is defined by

$$R(t) = I_N(t)/I_T(t), \quad (7)$$

where $I_T(t)$ is the total intensity of the fluorescence at time t and $I_N(t)$ is the intensity in the spectral band of initially excited ions with the interpolated background subtracted off.

In a recent paper,³⁰ a phenomenological model for $R(t)$ was developed which was based on coupled rate equations for the occupation probabilities of the various sites. Assuming that the transfer rate is independent of energy mismatch as in this case, the resulting (approximate) expression for $R(t)$ took the form

$$R(t) = \exp \sum_n (\ln \{ c [e^{-W_{0n}t} f_n(t) - 1] + 1 \}), \quad (8)$$

where W_{0n} is the transfer rate from site 0 to site n ($\approx W_{n0}$ for $kT >$ inhomogeneous linewidth, which is the case in all of our measurements) and c is the probability that site n is occupied by an optically active ion. The function $f_n(t)$ is 1 if back transfer is neglected altogether. As discussed in Ref. 30, a better approach is to take $f_n(t) = \cosh(W_{0n}t)$,

an approximation which treats back-transfer correctly at short times for all values of the concentration and gives the leading (order c) terms in the low-concentration limit for all values of the time. (See note added in proof.)

From (8) it is apparent that the time development of $R(t)$ depends in detail on how the transfer rate varies with the separation between the ions. A useful approximation is to assume that $W_{nn'}$ is proportional to an inverse power of the separation, viz,

$$W_{nn'} = (R_{\min}/r_{nn'})^s W_0, \quad (9)$$

where R_{\min} is the distance between nearest neighbors (2.733 Å in ruby), W_0 is the nominal nearest-neighbor transfer rate, and s is a parameter.

When the spectral transfer arises from multipolar interactions between ions, $s=6$ corresponds to dipole-dipole transfer, $s=8$ to dipole-quadrupole, $s=10$ to quadrupole-quadrupole, etc. In the case of exchange, where the transfer rate may depend strongly on the relative orientation of the pair of ions as well as on their separation, s characterizes the range of the angular average of the transfer rate.

For a dilute system we can replace the sum over n in Eq. (8) by an integral, thus, obtaining the result

$$\ln[1/R(t)] = \frac{4}{3} \pi^2 c^{3/s-1} n R_{\min}^3 (W_0 t)^{3/s} \Gamma(1-3/s), \quad (10)$$

for $f_n(t) = \cosh(W_{0n}t)$.³¹ Here n is the number of optically active ions per unit volume and $\Gamma(x)$ is the gamma function. Equation (10), as should be noted, does not hold at short times. In this limit discrete lattice effects become important and $R(t)$ varies as $\exp(-At)$ with $A = c \sum_n W_{0n}$.

In order to determine the appropriate value of s , we have plotted $\ln[I_T(t)/I_N(t)]$ on a log-log scale. Our results for the 0.9-at. % sample at 10 K are shown in Fig. 6. In the range 1–10 msec a least-squares fit indicates that $\ln[1/R(t)]$ varies as $1.16t^{3/10.8} + \text{const}$, from which we infer $s=10.8$. This value we obtain appears to rule out the dipole-dipole interaction as the dominant mechanism for spectral transfer, and is consistent with quadrupole-quadrupole transfer. However, according to estimates given by Birgeneau¹⁸ even at distances on the order of 13 Å (the average spacing between chromium ions for 0.9-at. % concentration), the quadrupole-quadrupole mechanism is much less important than exchange. Provided this is the case then our results indicate that the average of the transfer rate due to exchange varies in a manner similar to $r^{-10.8}$ for separations on the order of 10–15 Å.

Using Eq. (10) and the data shown in Fig. 6 we infer the value $W_0 = 6.9 \times 10^5 \text{ msec}^{-1}$, a result

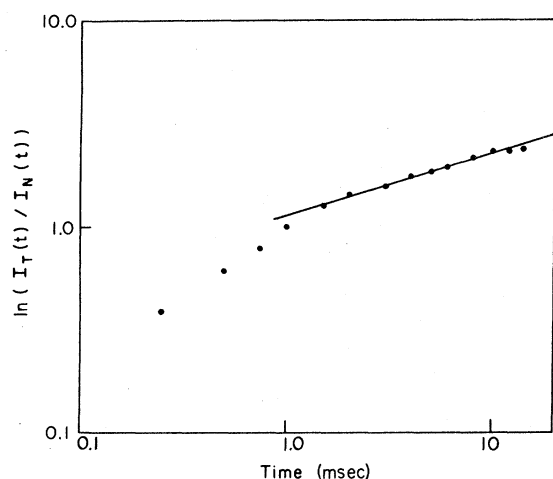


FIG. 6. Log-log plot of $\ln [1/R(t)]$ (defined in text) vs time, for the 0.9-at. % sample at 10 K. Straight line is a least-squares fit to the data after 1 msec.

which is in reasonable agreement with a direct calculation using Eq. (8) and carrying out the summation over the sites of the corundum lattice (see Fig. 7).³² With this value of W_0 we obtain from Eq. (9) a transfer time of 30 msec between pairs of ions separated by 13 Å. This time is significantly greater than the "characteristic" energy-transfer time defined in Sec. IVA, which is on the order of 1 msec. However, it is clear from Eq. (10) that for a given concentration the characteristic transfer time of Sec. IVA and the pair-transfer time are proportional to one another. As a consequence, inferences about the temperature dependence of the characteristic transfer times apply equally well to the pair-transfer times.

By making use of Eq. (2) and the above pair-

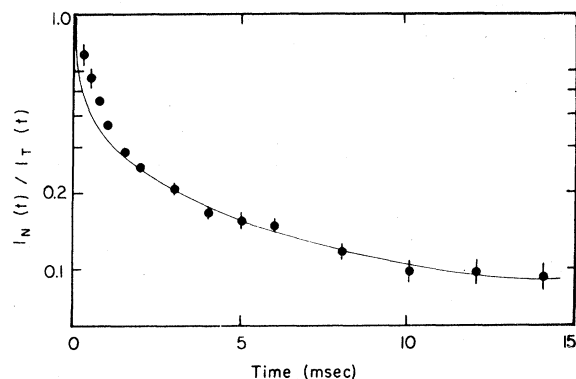


FIG. 7. Linear plot of $R(t)$ vs time for the same data used in Fig. 6. The curve is a best fit using the values $s = 10.8$ and $W_0 = 1.1 \times 10^6 \text{ msec}^{-1}$ in Eq. (8). A sum is performed over the discrete points of the corundum lattice, starting from a distance of 5 Å (nearer ions are assumed to be coupled into pairs and therefore are not part of the R_1 spectrum).

transfer rate, we can obtain a crude estimate of the coupling between ions 13 Å apart. With $\Delta M^{(1)} - \Delta M^{(2)} = 5 \times 10^3 \text{ cm}^{-1}$, $\rho = 4 \text{ g cm}^{-3}$, and $v^5 = 1.6 \times 10^{29} \text{ cm}^5 \text{ sec}^{-5}$, we find $J_{1,2} \approx 2 \times 10^{-3} \text{ cm}^{-1}$. This value is more than three orders of magnitude greater than the estimated strength of the quadrupole coupling, $6 \times 10^{-7} \text{ cm}^{-1}$, given in Ref. 18. On the basis of this comparison we conclude that the transfer probably arises from a long range ($\sim 10\text{--}15 \text{ Å}$) component of the exchange interaction between ions.

As noted, the functional form shown in Eq. (10) is not applicable at short times, as is evident in Fig. 6. The increase in slope below 1 msec is consistent with a crossover from linear behavior at short times [$R(t) \approx \exp(-At)$] to a $t^{3/5}$ variation at longer times.

C. Radiative spectral transfer

In addition to nonradiative spectral transfer, radiative transfer also occurs in macroscopic samples where the crystal dimensions exceed the photon mean free path. The process of phonon-assisted radiative transfer has been examined theoretically by Holstein, Lyo, and Orbach,³³ and experimental evidence in ruby supporting their predictions has been recently provided by Selzer and Yen.¹² The experimental results and a comparison with the theory have been covered in Ref. 12, and only a few additional details are provided below.

At lower temperatures where the feeding rate was very slow, an extrapolation process was used to obtain the characteristic rate, once again defined as the $1/e$ point in the narrowed-to-total-intensity ratio, for direct comparison with the "characteristic" nonradiative rates. It has been found that for nonradiative transfer, a linear contraction of the time scale with increasing temperature will cause all the curves of the type shown in Fig. 7 to coincide—i.e., the shape of the $I_N(t)/I_T(t)$ curves do not change with temperature. Similarly, curves of this same ratio for the radiative-transfer data also appear to have a universal shape (but the large scatter in the data due to the weak signals prevents the extraction of any meaningful functional dependence in this case). A curve for the time development of the maximum observed rate at 42 K is shown in Fig. 8.

Below 25 K, the $1/e$ ratio of $I_N(t)/I_T(t)$ could never be reached before the signal-to-noise ratio became impractically small. Hence, at these temperatures a number of data points were fit to the curve shown in Fig. 8 using an appropriately expanded time scale, and the $1/e$ time of the original curve multiplied by the scale factor to give

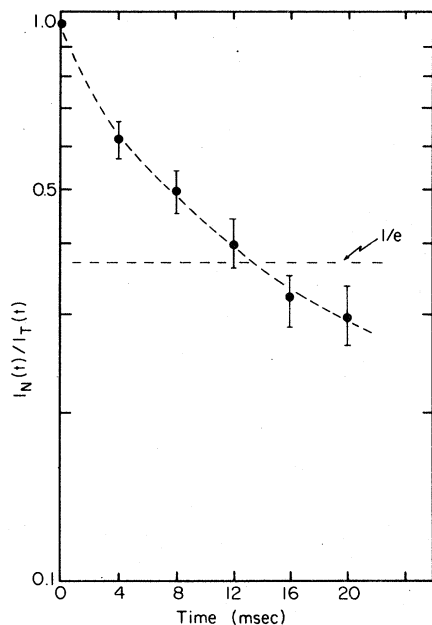


FIG. 8. Semilog plot of $R(t)$ vs time for the radiative transfer data of Ref. 12. The "characteristic" transfer time is seen to be approximately 13 msec.

the transfer time. A plot of the transfer rate (inverse transfer time) obtained in this way versus T is also shown in Ref. 12. Even with the large relative error inherent in this fitting process, the data are certainly more consistent with an exponential than with a linear fit.

Reference 12 also reports the observation of resonant radiative transfer, which is manifested as a line separated in energy from the resonance fluorescence line by twice the ground-state splitting (either higher or lower in energy, depending on which side of the line is excited by the laser) which is observed to grow in time. For higher concentrations, the effect is also observed, but in this case there will be three narrowed components at $t=0$, one on each side of the resonance line as discussed in Sec. III, and the transfer appears as the growth of a fourth line.

For a given geometry, if we can assume that the resonant transfer at a given excitation frequency has a fixed rate W_x , then the transfer process between the donors (A sites) and acceptors (B sites) can be described by the rate equations

$$\frac{dN_d}{dt} = -W_r N_d + W_x N_a, \quad \frac{dN_a}{dt} = -W_r N_a + W_x N_d, \quad (11)$$

where N_d and N_a are the donor and acceptor populations, and W_r is the radiative-decay rate. Taking the initial conditions to be $N_d = N_0$ and $N_a = 0$, these equations yield the following decay curves:

$$N_d(t) = \frac{1}{2} N_0 (e^{-(W_r - W_x)t} + e^{-(W_r + W_x)t}), \quad (12)$$

$$N_a(t) = \frac{1}{2} N_0 (e^{-(W_r - W_x)t} - e^{-(W_r + W_x)t}). \quad (13)$$

From the measured broadband lifetime, $N_d(t) + N_a(t)$, and the knowledge of W_r [$(3.6 \text{ msec})^{-1}$ is the generally accepted value], it is possible to extract W_x and having this value, compare the experimental rise of the acceptor line with that predicted by Eq. (13). For the data shown in Fig. 3, Ref. 12, the broadband lifetime was found to be 5.5 msec, yielding a radiative transfer rate of $W_x = 0.096 \text{ msec}^{-1}$ and a predicted risetime of 2.67 msec for the third line. This compares favorably with the measured value of $2.3 \pm 0.4 \text{ msec}$. Thus, the rise of the third peak can be adequately described by the proposed resonant radiative transfer model.

D. Interline nonradiative transfer

In addition to the spectral transfer within the inhomogeneous line discussed in A, it is well known that there also exists a flux of energy from excited Cr ions to the various exchange coupled Cr pairs.⁵ However, the nature of this energy transfer is still controversial, with two different models being supported by different groups.^{5,10,34-36} One model presumes a very rapid transfer of energy between isolated Cr ions (R ions) until the excitation migrates to a pair (N line) and transfers via emission of a $\sim 100\text{-cm}^{-1}$ photon. The slowest rate in this process would be the $R \rightarrow N$ transfer. The other model assumes a rapid $R \rightarrow N$ transfer and a considerably slower or even nonexistent $R \rightarrow R$ transfer. Both models appear to have supporting experimental evidence, including the recent heat-pulse experiments by Heber and Murmann (HM)³⁷ which favor the latter.

We believe that our FLN and time-resolved experiments in conjunction with other published results might resolve the controversy over the R to N transfer. However, the picture that evolves is complex and requires a rather detailed chain of reasoning.

After exciting the R line in the same fashion as for the spectral-transfer measurements, fluorescence from one or the other of the two strongest pair lines (N_2 at 7009 \AA and N_1 at 7041 \AA) has been studied. The emission in all cases seems to have a complex initial rise which is a function of pump frequency within the R line, followed by an exponential tail at the R line lifetime. This general behavior is independent of temperature down to 5 K (the lowest temperature at which these measurements were made), and is only weakly dependent on concentration between 0.08 and 0.9 at. %.

Since the feeding of the N lines occurs at tem-

peratures and concentrations where no or very slow spectral transfer of the type discussed in A is detected we conclude that either there is no transfer between R ions before the $R \rightarrow N$ transfer (assuming that the $R-R$ transfer occurs only via the one-phonon-assisted process), or else a distinct, resonant process between R ions must also be present—one which transfers spatially without shifting frequency.

If there is no $R-R$ transfer before the $R \rightarrow N$ transition, then the behavior of the system should be properly described by a simple rate-equation analysis. If we assume that a given donor can feed only one acceptor, but a given acceptor can be fed by any number of donors, we arrive at the expressions for the donor (R line) and acceptor (N line) fluorescence as a function of time after excitation into the R line

$$N_d = \sum_i N_0 e^{-(w_R + w_{R \rightarrow N}^{(i)})t}$$

$$N_a = N_0 \sum_i \frac{W_{R \rightarrow N}^{(i)}}{W_N - (W_R + W_{R \rightarrow N}^{(i)})} \times (e^{-(w_R + w_{R \rightarrow N}^{(i)})t} - e^{-w_N t}), \quad (14)$$

where W_R and W_N are the intrinsic decay rates of the R and N lines, and $W_{R \rightarrow N}$ is the transfer rate. If $W_{R \rightarrow N}$ is considerably smaller than W_R and W_N , these equations reduce to the following approximations:

$$N_d \approx N_0 e^{-w_R t},$$

$$N_a \approx N_0 \sum_i \frac{W_{R \rightarrow N}^{(i)}}{W_N - W_R} (e^{-w_R t} - e^{-w_N t}), \quad (15)$$

In this case, the R -line lifetime would not show any deviation from its intrinsic exponential rate, and the N line would exhibit a simple two-exponential development, with the tail at the R -line lifetime. However, as soon as $W_{R \rightarrow N}$ becomes large enough to influence the R -line lifetime, then nonexponential behavior would ensue for both the R -line and N -line tail.

In order to test whether Eqs. (14) or (15) appropriately describe this system, lifetime measurements were made on ruby powders (with low resolution, to encompass the entire inhomogeneous line), where the influence of radiative trapping could be eliminated, or at least significantly reduced. At a concentration of 0.5 at. % the R -line lifetime at 5 K was found to have shortened from 3.6 to 2.8 ± 0.1 msec, indicating the presence of a nonvanishing $W_{R \rightarrow N}$. Yet, as shown in Fig. 9, both the R -line lifetime and the tail of the N line show a strictly exponential time

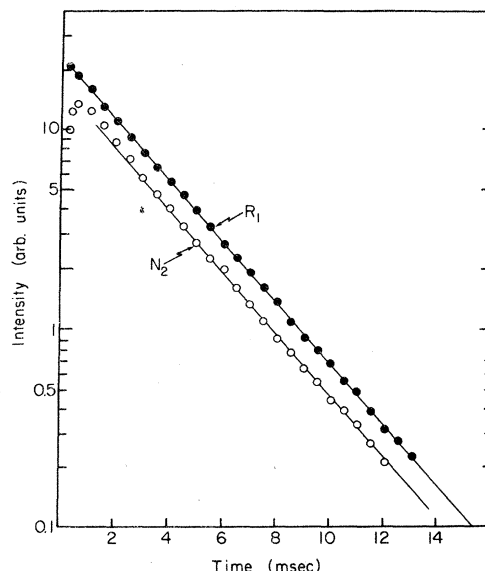


FIG. 9. Semilog plot of broadband (1-nm resolution) R_1 and N_2 lifetimes for a 0.51 at. % powdered sample at 5 K. The straight lines represent a decay time of 2.8 msec. Laser excitation is slightly on the high-energy side of line center.

dependence—in the case of the R line for approximately five e folds, starting as close in as 0.2 msec after the laser pulse.³⁸ This behavior is inconsistent with Eqs. (14) and (15), and, as we shall see, supports the model of rapid transfer within the R line.

Basic to the rapid-transfer model is the assumption that the $R-R$ transfer rate must be fast enough to effectively average over all possible configurations, thereby leading to a single, characteristic rate constant for $W_{R \rightarrow N}$. With this assumption, the expressions for donor and acceptor decays become particularly simple³⁶:

$$N_d = N_0 e^{-(w_R + w_{R \rightarrow N})t}, \quad (16)$$

$$N_a = N_0 \frac{W_{R \rightarrow N}}{W_N - (W_R + W_{R \rightarrow N})} \times (e^{-(w_R + w_{R \rightarrow N})t} - e^{-w_N t}). \quad (17)$$

The R line should have an exponential decay, and the N line, an exponential rise at its intrinsic lifetime followed by a tail at the R -line decay rate.

The exponential R -line decay with a rate significantly faster than its intrinsic lifetime, and the N -line tail at the same rate are clearly consistent with these equations. However, additional complexities occur. The rise of the N line is not always exponential and is faster than the expected value (which is 0.7 msec for the N_2 -line as determined by exciting this pair directly). Furthermore, the initial risetime varies as a function of

laser-excitation frequency. From this behavior and the recent results of HM and others,³⁴⁻³⁶ it is apparent that this simple model involving only three rate constants is insufficient to adequately describe this system. We therefore have sought additional evidence which would allow a consistent interpretation of the various, seemingly contradictory results.

Particularly illuminating are the HM results of Ref. 37. In this experiment, the N_2 line is pumped at low temperatures with a pulsed dye laser, and then a short heat pulse is applied to effect transfer back to the R lines. Decay of the fluorescence originating from the vicinity of the R lines is then monitored after termination of the heat pulse. If the simple three-rate model described by Eqs. (16) and (17) were correct, then the R line, after transfer from the pair via the heat pulse, would decay at the same intrinsic rate measured when it is excited directly (approximately 4 msec), rather than the much faster rates observed by the authors. However, the "diffusion-limited" model (proposed by the authors to explain their results)—slow $R \rightarrow R$ diffusion ($\sim 250 \mu\text{sec}$) and fast $R \rightarrow N$ transfer ($\sim 4 \mu\text{sec}$)—is inconsistent with the exponential lifetimes and the very slow intraline transfer rates observed in our samples below 10 K.

A revealing clue to solve this apparent contradiction is the fact that in the HM experiment, only those ions which couple strongly to the pairs (presumably fairly near neighbors to the pair) and which fluorescence in the vicinity of the R lines (the experiment was performed with very low resolution) are excited by the heat pulse. We propose that these ions, because of their proximity to the pair, are themselves unique—neither truly isolated nor tightly bound into a triplet. These ions, which we henceforth refer to as R' ions, couple strongly to the pair but only weakly to the isolated R ions. In the HM experiment, it was the fluorescence from these R' ions not the R ions, which was monitored.

To test this hypothesis, a search was made for ions with levels in the vicinity of the R line which couple rapidly to the various pairs. These experiments were performed by selective excitation of the different pair lines at very short delays. The laser was scanned in the region between R_2 and R_1 while the pair fluorescence was measured with a boxcar integrator, having a $5 \mu\text{sec}$ delay and a $1 \mu\text{sec}$ gate width. Transfer of the type shown in Fig. 9 and in Fig. 3 of Ref. 11 would not be observed on this type of a scan because the intensity of the pair increases from zero relatively slowly. Only the position of ions which couple rapidly to the pair or excited levels of the pair itself would be revealed. Figure 10 shows selective excitation

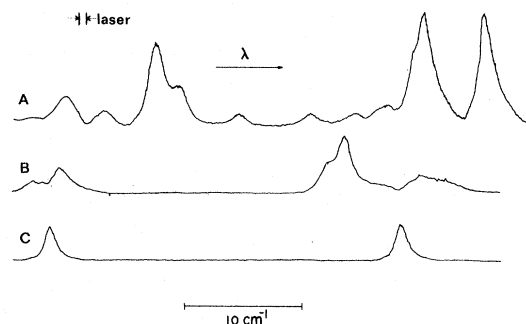


FIG. 10. Selective excitation scans of the N_2 and N_1 lines (A and B, respectively) at 6 K for the 0.51-at. % crystal, with the laser scanning the region between R_2 and R_1 . A and B are taken at 5- μsec delay and trace C (the N_2 line), at 3 msec. The gain settings are roughly the same for all traces. For these scans, the intracavity laser etalon was removed.

scans for the two strong pair lines at 6 K. Also included is a scan of the 7009 Å pair at a 3-msec delay. The short delay scans reveal a number of reproducible bumps which indicate rapid channels of excitation of the different pairs. While two or three lines assumed to be excited states of the N_2 pair have been noted in the vicinity of the R lines (and none for the N_1 pair in this same region³⁹) we believe that these could not all be excited pair states. If they were, the stronger lines could easily have been identified as belonging to N_1 or N_2 by the methods used in Ref. 39, rather than being labeled as "distant" pairs. The fact that the strongest of the lines in Fig. 10 are separated by approximately the same splitting as the R lines (29 cm^{-1}) further supports our hypothesis that these lines originate from strongly perturbed Cr ions, near to but not part of a pair. These, then, are the R' ions which were excited in the HM experiment and which showed the rapid decays, not the truly isolated Cr ions, which fluoresce at R_1 and R_2 . This interpretation differs from that of Ref. 34, wherein a line presumably coincident with an R' level is identified as a delocalized exciton band.

When the R' ions are excited directly by the laser, no resonance fluorescence is observed, and the appropriate pair line shows an immediate rise (limited by the roughly $1 \mu\text{sec}$ response of our electronics) followed by an exponential decay at either 0.7 or 1.1 msec for N_2 or N_1 , respectively. These are the same lifetimes observed when exciting directly into the fluorescing levels of the pairs themselves.

The excitation scan taken at a 3-msec delay reveals ions which couple more weakly to the pairs with the process depicted in Fig. 9 and in Fig. 3 of Ref. 11; i.e., having a slow rise and a tail at the R -line lifetime. As expected, these peaks coincide with the position and width of the R_1 and R_2 lines.

None of the other peaks are observed since by 3 msec, the N -line fluorescence has decayed considerably after "direct" excitation into the R' ions.

Additional evidence supporting the existence of R' ions has been provided in two ways. At a temperature of 120 K, the fluorescing level of the N_2 line at $14\,299\text{ cm}^{-1}$ was excited directly by the laser and fluorescence in the vicinity of the R lines monitored. This would correspond to the HM experiment, only with an infinitely long heat pulse. With the spectrometer tuned to the position of the most intense R' lines, slightly lower in energy than the R lines (see trace A, Fig. 10), a 0.7-msec decay is observed. Tuning the spectrometer to the center of the R line, a weaker decay at approximately 4 msec is seen. The two lines overlap too strongly, however, to observe any possible rise to the R line, which would be expected. Clearly, the R' ions are in thermal equilibrium with the pairs, but the R ions are not. Hence, the coupling between R ions and R' ions must also be weak—most likely the same one-phonon process as described in Sec. IV A for transfer from the narrowed component to the background.

Line-narrowing experiments of the N_2 pair line have also been performed for the 0.5-at. % sample at low temperatures when pumping into various excitation channels. No narrowing of the pair is seen when the center of the R line is pumped: i.e., the full inhomogeneous width of approximately 2 cm^{-1} is observed in fluorescence. When any of the R' lines are excited, a slight narrowing of approximately 15% is seen. However when the $14\,299\text{-cm}^{-1}$ level is pumped directly, the fluorescence narrows to approximately 0.7 cm^{-1} . These results suggest that only slight site selection is obtained by pumping into the R' ions because although they are spatially near the pairs, they are not necessarily in the identical strain environment. If the R' lines are really higher-lying levels of the pair, greater line narrowing would have been expected when they are excited. Because of the complications associated with line narrowing of nonresonant transitions,^{13,14} and also the likelihood of a significant homogeneous component to these lines from phonon-induced relaxation between ground-state levels, these line-narrowing results are in themselves not entirely conclusive, but are only consistent with the proposed model.

Finally, a complete model must be able to explain the roughly 500- μ sec tail of the " R -line" decay in the HM experiment after the heat pulse and the comparable rate for the initial rise of the N_2 line after exciting the R_1 line in our experi-

ments (see Fig. 9). If both these rates were 700 μ sec rather than 500 μ sec, they would presumably be reflecting the intrinsic-pair lifetime. This then would be consistent with Eq. (17) for rapid transfer and also with the likely possibility of residual heating from the pulse in the HM experiment, since the return to thermal equilibrium is quite slow.⁴⁰ However, the 40% difference in these rates is considerably larger than our experimental error, and must be taken as significant. We therefore propose that in addition to the R' ions which couple very strongly to the pairs and have energy levels shifted from the R line, there also exist R'' ions. These ions would couple more weakly to the pair, in the vicinity of 300–400 μ sec, and would have absorption levels shifted immeasurably from the R lines. Both R' and R'' ions would be excited in the heat-pulse experiment, the latter giving rise to the longer tail. The R'' would also be excited directly by the laser in our experiments and would therefore combine with the 700- μ sec pair decay to give the observed \sim 500- μ sec feeding of the N_2 pair. Note that the N_1 pair shows a rise at a roughly exponential rate of 0.7 μ sec whereas this pair has a lifetime of 1.1 msec. With normal scatter of the data, it would be very difficult to detect the slight deviations from the exponential rate expected for this type of behavior.

Because of the very short-range and highly anisotropic nature of the superexchange interaction,⁴¹ the discrete nature of the R' and R'' ions is made more plausible. These ions could be nearly equidistant from the pair and yet have coupling strengths which differ vastly. A position even closer could result in the formation of a triplet, and one more distant might have a vanishingly small interaction.

In summary, the equal exponential decays of the R -line and the N -line tail are explained by rapid R - R transfer which averages over distance and gives rise to a single rate constant. This constant, which we originally labeled as $W_{R \rightarrow N}$, should more properly be called $W_{R \rightarrow R'}$, and is the slowest rate in the transfer process. The complex rise of the N line is due to the feeding of the pairs both directly by the excited R'' ions (and some R' ions when the R and R' absorptions overlap) as well as indirectly via the $R \rightarrow R' \rightarrow N$ process.

A final comment might be made about the lifetime measurements of Ref. 35. Using flashlamp excitation, the author obtained nonexponential decays of the R line between 0 and 2 msec; however, no data were obtained beyond this delay. In the high concentrations that he examined, a nonexponential *initial* decay is plausible due to the presence of the various types of R ions, all excited simul-

taneously by his broadband pump. However, the tail of this line after delays long enough for the R population to become negligible would still be expected to exhibit exponential behavior.

E. Anderson localization and ruby

With the demonstration of energy transfer between single Cr ions and pairs,⁵ ruby has been proposed as a possible candidate for "Anderson localization." Anderson showed⁴² that in random inhomogeneously broadened systems where the ion-ion interaction strength falls off more rapidly than r^{-3} (where r is the interion separation), a critical concentration should exist. Below this concentration, the system would be localized, with no transfer of energy between ions, and above this concentration a conducting state would exist, with rapid energy migration. The conduction of energy is assumed to be a coherent process—that is, an excitonlike state, involving resonant ions fulfilling the condition $\Delta E_{1,2} \leq J_{1,2}$, where ΔE is the energy mismatch and J is the coupling strength of the interacting ions. Even in the localized state, incoherent phonon-assisted processes of the type discussed in Sec. IV A can produce energy migration at elevated temperatures,²¹ but the onset of conduction (or localization) depends only on concentration.⁴³

Because the interaction between Cr ions in ruby is assumed to be exchange, which is shorter range than r^{-3} , ruby might be expected to exhibit localization. Lyo⁶ has calculated that the critical concentration should be in range of 0.3- to 0.4-at.% Cr, below which no rapid, coherent energy migration would occur. However, a number of approximations were employed in the derivation—rectangular density of states, fixed inhomogeneous width for different concentrations, and an exchange interaction only very approximately known. Thus, according to the author, the value for critical concentration is but a rough estimate.

It should be emphasized that the concept of Anderson localization requires microscopic strain broadening. In the conducting regime, ions which are closer spatially but statistically farther apart in energy can still interact (as long as $J > \Delta E$) because of the strong dependence of J on spatial separation. If the strains are nonrandom on a microscopic scale so that regions exist where ions are all nearly in resonance, conduction among these ions can occur to very low concentrations and in fact, the condition for localization may never be met.

In a recent experiment, Koo, Walker, and Geschwind¹⁰ (KWG) believe to have supporting evidence for Anderson localization in ruby with

their observation of "mobility edges": The authors detected a rather abrupt decrease in the ratio of the pair to the single-ion fluorescence intensity as a high-resolution laser was scanned from line center toward the low-energy side of the inhomogeneous R_1 absorption.

This concept of a mobility edge is easy to conceptualize for a sample just above the critical concentration: Since the inhomogeneous line for a totally random system is presumed to reflect only the number density of ions with a given energy-level spacing, at line center the density of ions is greatest and hence the average distance between them is least. Toward the edge of the line, the number of ions with levels at a given energy falls off, and therefore the average distance between them increases. At some point in the wings of the line, the critical condition for Anderson localization will be met for ions with that particular energy. They are no longer able to transfer the excitation to other ions of the same energy because there are just too few. If these or other ions further in the wing are excited with a high-resolution laser, no conduction would be expected, but with the excitation closer to line center, the conducting state would exist.

Our results obtained for the $R \rightarrow N$ and $R \rightarrow$ background transfer (Secs. IV D and IV A respectively) do not dispute the possibility of the conducting state. In fact, for the 0.5-at.% sample for which the most $R \rightarrow N$ data were taken, a rapid, resonant transfer is presumably required in order to explain the lifetime data. Yet, it is difficult to reconcile the totality of our results with microscopic strains and, hence, with the possibility of localization. We believe that a strong case for macroscopic rather than microscopic broadening was made in Ref. 12 with the observation of resonant radiative transfer (a long-range process) and yet a presumed lack of resonant nonradiative transfer (a short-range process) between the A and B sites. While the assumption of microscopic random strains has greatly simplified calculations on ruby, the suggestion of either nonrandom strains or Cr distribution has been proposed by several authors,^{5,9,11,12,44} particularly in flame-fusions samples. As yet there has been no direct verification of the strain distribution in ruby, but it appears that a number of rather diverse experiments can be better explained without the assumption of microscopic randomness.

In addition, our experiments have demonstrated that the inhomogeneous R_1 line of ruby, rather than indicating the random distribution of energy levels presumed necessary for the existence of a mobility edge, is a composite of different types of Cr ions: some strongly coupled to discrete

pairs, others associated with weak clusters, and still others which can be thought of as truly isolated. We question whether the interpretation of a mobility edge is justified in light of this complex structure. Furthermore, none of our experiments performed on samples in the range of 0.08–0.5 at. %, where according to Ref. 10 there should be a mobility edge, have revealed any discontinuous behavior in energy-transfer properties as a function of laser pump frequency. Thus, we can find no evidence in the intraline transfer for effects which might be attributed to differences among the localized-to-localized, localized-to-conducting, and conducting-to-conducting transfer rates.

What then is the source of the phenomenon observed in the KWG experiment? We can only speculate that the change in intensity ratio may signal the transition between “normal” and “abnormal” ions of the type discussed in Sec. III. It should be noted that the KWG experiments were performed only on the low-energy side of the line, where the abnormal ions are more abundant, as reflected in Fig. 4.

Finally, we have also observed that the inhomogeneous linewidths for the powders we have examined are invariably larger than those of the crystals from which they were made, sometimes by as much as a factor of 2 or 3. Since crushing would not be likely to introduce microscopic strains, it is highly probable that powders exhibit macroscopic broadening, with some of the grains strained differently than others. These results cast further doubt upon the existence of a mobility edge in ruby. However, an alternative explanation for the KWG results must await further experimentation.

V. DISCUSSION

The results of our various measurements on ruby may be summarized as follows:

(i) Linewidth measurements of the resonance fluorescence component show a very large increase in linewidth in the wings of the inhomogeneous absorption, particularly on the low-energy side. This phenomenon is presumed to be evidence for weak clustering of Cr ions resulting in unresolved splitting of the energy levels.

(ii) At concentrations above roughly 0.05 at. %, a nonradiative spectral transfer occurs between ions excited by the laser and those which fluoresce at frequencies approximating the full inhomogeneous background. The temperature and frequency dependence of the process are consistent with a one-phonon direct transfer, although theoretical pre-

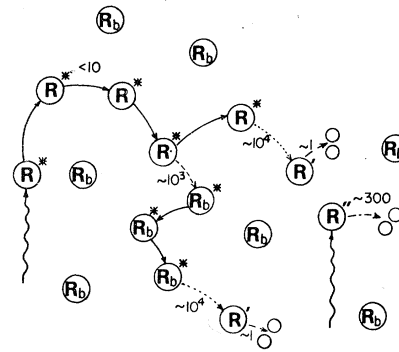


FIG. 11. Model of energy transfer in ruby (explained in the text). R^* refers to those ions in resonance with the laser frequency, R_b to those at different energies within the inhomogeneous background, and R' to a resonant group of background ions. Various channels of energy migration are indicated with the approximate transfer times (derived from our different experiments) given in microseconds.

dictions favor a higher-order process.

(iii) Below this concentration, spectral energy transfer can be dominated by a radiative process if the samples are large enough to trap photons effectively. The temperature dependence of the radiative transfer is consistent with a two-phonon “resonant” process involving the $2\bar{A}$ level.

(iv) Low-resolution lifetime measurements of the R_1 line at all temperatures exhibit exponential decays which for concentrations above 0.3 at. % exceed the intrinsic R_1 decay rate of (3.6 msec).⁻¹ The N -line lifetimes show an initial rise which depends on the laser pump frequency, followed by an exponential tail at the R_1 decay rate. The exponential behavior supports a rapid energy transfer between resonant Cr ions.

(v) Selective excitation scans of the N_1 and N_2 pair lines while tuning the laser in the vicinity of the R lines revealed numerous channels for rapidly feeding the pairs, which are different for the different pairs. These channels are postulated to be Cr ions near enough to the pair to have perturbed 2E levels but not close enough to form a “triplet.”

The model which we propose to explain the (non-radiative) energy transfer phenomena in ruby can be visualized as in Fig. 11. Here we show one photon absorbed by an isolated Cr ion in resonance with the laser, labeled R^* , and another absorbed by an R' ion, also in resonance with the laser but in the proximity of and coupling strongly to a pair.

The excitation travels rapidly (at a rate sufficiently fast to average over distance) along a chain of resonant R^* ions until it reaches an R' ion—one neighboring the pair in a highly perturbed environment. The transition between R^* and R' most like-

ly involves the emission of a long-wavelength phonon, and from the shortening of the R_1 lifetime, we deduce this rate to be approximately 10 msec at 5 K and faster at higher temperatures.⁴⁵ Once on R' , the excitation is very rapidly channeled to the pair.

Alternatively, the excitation can transfer non-resonantly from an R^* ion to one with a different energy level within the inhomogeneous background, labeled R_b^* . From here, it can travel resonantly between different R_b^* ions until it is again in the proximity of an R' ion near a (different) trap. (It is statistically unlikely that a given pair would be adjacent to more than one R' or R'' ion.) It is also conceivable that the R'' ions are in some instances fed resonantly by a chain of R^* ions. However, this would not alter the observed rise of the N lines. Furthermore, from the strictly exponential decay of the R line in our samples, it is apparent that the number of R'' ions (or ions which couple resonantly to the R'' ions) constitute only a very small fraction of the total R ions at concentrations below 0.5 at. %.

While this model may account for the various experimental observations made by ourselves and others, it is necessary for self-consistency to reconcile the observed spectral transfer of Sec. IV A with the proposed rapid spatial transfer required to explain the lifetime data. The localized-state point of view has been shown in Sec. IV B to adequately describe the time development of the intraline transfer, and the predominance of delocalized states could considerably alter this behavior. Why does the assumed mobility of the excitation not also lead to exponential decays of the narrowed component, indicating a fixed $R^*-R_b^*$ rate at some average distance?

We are unable to give a definitive answer to this question. However, we can make the self-consistency of our interpretation of the spectral and spatial transfer at least plausible.

As already noted, the most significant difference between the R^* -to-background and the R^* -to- R' transfer is that the latter is characterized by approximately exponential [$\exp(-At)$] decay, whereas the former deviates appreciably from exponential behavior in a manner described by Eq. (10). Provided we neglect back-transfer effects, which is permissible for short times, we can characterize both processes by a general expression of the form

$$I_N(t) \propto \sum_{\alpha} \exp(-W_R t - \sum_{\beta} W_{\alpha\beta} t), \quad (18)$$

where, as before, $I_N(t)$ denotes the intensity of the narrowed component and W_R is the radiative-decay rate. The symbol α denotes the states initially

excited by the laser pulse, β denotes the other states of the system, and $W_{\alpha\beta}$ is the transition rate from state α to state β . At low temperatures, where the R^* -to- R' transfer is dominant, β refers to states localized at the site of the R' ions. In situations where spectral transfer is dominant, β refers to extended states whose energies span the inhomogeneous line. (By "extended state" we mean a state where the wave function has significant amplitude at a number of sites. It need not be a state of infinite extent like an exciton in a periodic array of ions.)

From the near-exponential decay of the R line in the presence of significant R -to- N transfer we can conclude that the spatial extent of the extended states must be such that their characteristic dimensions are at least as large as the typical spacing between different exchange-coupled pairs. Were this not the case, a significant fraction of R^* ions would decay with the radiative lifetime, and the corresponding form for $I_N(t)$ would then be

$$I_N(t) = n_{A1} \exp[-(W_R + W_{RR'})t] + n_{A2} \exp(-W_R t), \quad (19)$$

where n_{A1} (n_{A2}) is the number of initially excited ions that do (do not) transfer to pairs. The presence of exponential decay implies that the distribution in rates for transfer from the extended states to the R' ions is sharply peaked about some mean value different from zero. The most reasonable explanation for this peaking appears to lie in the range of the interaction coupling the extended states to the localized levels. If the interaction has a short range then transfer from R^* to R' will take place largely from sites which are "nearest" to the R' ions. As a consequence the "nearest" transfer rate will dominate the distribution.

The nonexponential behavior seen in the R^* to R_b^* reflects a much broader distribution in transfer rates. This aspect of the data is not surprising since the transfer is taking place to a continuum of states involving various configurations of quasi-degenerate ions. What is surprising is that for $t > 1$ msec, the decay is adequately described by Eq. (10), which would appear to imply transfer between states confined to single sites. However, this need not be the case. Although in the limit $c \ll 1$, Eq. (8), which is based on the local site picture, reduces to Eq. (10) [with a transfer rate of the form shown in Eq. (9)], the latter equation could just as well have been derived without reference to the underlying lattice structure, as was originally done by Inokuti and Hirayama.³¹ As such it is equally applicable to extended states provided the transfer rate between states has the form shown in Eq. (9), with r_{mn} being interpreted as the distance between the "centers of gravity" of the two states, and N as the number of states

per unit volume. (The position of the "center of gravity," $\bar{R}_{c.m.}$, is given by $\sum_n \vec{r}_n |a_n|^2$ where a_n is the amplitude of the single ion state at \vec{r}_n which appears in the expansion of the extended state wave function.) Although this argument makes the origin of the $t^{3/2}$ behavior for transfer between extended states more plausible, there are still many questions left. In particular, it is not obvious why the effective average transfer rate between extended states should have a simple inverse power dependence on the separation between their centers of gravity.

Finally, we note that if the extended-state picture is valid, then the parameter W_0 in Eq. (9) which was found to have a value of $6.9 \times 10^5 \text{ msec}^{-1}$ on the basis of localized-state transfer, has to be interpreted as an effective site-to-site transfer rate.

It should be reemphasized that our assumption of rapid resonant-energy transfer (or delocalized states) is based on the exponential decay of the R_1 line at a rate faster than the radiative lifetime. If this behavior could be explained *without* resorting to an additional, average transfer rate $W_{R^*-R^*}$, then evidence for resonant transfer would no longer be as compelling, and the transfer process below a concentration of 0.9 at % could be explained by the localized picture of Eq. (15).

For example, if the addition of Cr^{3+} in the corundum lattice would sufficiently distort the lattice so that the site symmetry alters slightly as a function of increasing Cr concentration, then the observed decrease of the R_1 lifetime would merely reflect a change in oscillator strength of the $\bar{E} \rightarrow {}^4A_2$ transition. It is unlikely, however, that such an effect should be observed at low concentrations. Furthermore, any lattice distortion sufficient to change the oscillator strength by almost 25% (a reduction of τ_R from 3.6 to 2.8 msec) would presumably also produce an increase in the splittings of the 4A_2 and 2E levels as well as in the inhomogeneous linewidths. No such changes in energy-level splittings have been detected at high Cr concentrations, and the continuous increase in inhomogeneous width with concentration seems to be uncorrelated to the rather abrupt decrease in lifetime in the vicinity of 0.5 at %.

It is also unlikely that such a large reduction of the lifetime could result from the weak clustering discussed in Sec. III, particularly with the laser excitation near line center or on the high-energy side where the clustering would not be very prevalent. Once again an exchange coupling sufficient to produce a significant increase in oscillator strength should also produce noticeable alterations in the energy level structure.⁴⁶ Thus, at present, we can conceive of no other viable explanation for

the reduction of the R_1 decay besides the proposed resonant transfer mechanism.

VI. CONCLUSION

It should be clear from the foregoing discussion that our understanding of ruby is still far from complete. Very little information is presently available about the nature of strain broadening in these ionic crystals. Our results favor macroscopic broadening, but this can occur in a multitude of different ways, each of which may lead to different spectral dynamics. Strains which vary slowly and continuously throughout the crystal could presumably not account for the rise of the full background line shape, as reported in Sec. IV A. Rather, a gradual spreading of the narrowed component would be expected. A structure more likely to produce the observed narrowed-to-background and R -to- N transfer would consist of microscopic domains or perhaps one-dimensional chains in which all of the R ions are in near resonance, separated from each other by rather abrupt changes in strain environment. But is this type of structure to be reasonably expected from the crystal-growth process, and how large might these domains be? Comparison of our results with the spectral dynamics in ruby samples grown by methods other than flame fusion, or of Cr in other host materials may help clarify these questions.

The nature of resonant transfer in ruby is also uncertain. Is it a truly coherent process or an incoherent one between near resonant ions, W_{res} from Eq. (3), which is enhanced by a nonrandom energy distribution? Techniques which examine the decay of a coherently prepared state, such as photon echoes⁷ or laser-frequency switching,⁴⁷ may provide an answer, although results obtained on ruby to date show large systematic differences in echo decay times as a function of the experimental method employed.⁴⁸ Since the coherence times in ruby are known to be strongly magnetic field dependent,^{7,48} a study of the energy transfer in an applied field might also reveal important clues about the transfer mechanism.

The existence of Anderson localization in ruby or any other impurity-ion system still remains to be demonstrated conclusively. A search for mobility edges on both sides of the inhomogeneous line in very carefully prepared (perhaps annealed and etched) ruby powders, or in other simpler systems (if any exist) may prove enlightening. Note that the delocalized state signified by a mobility edge would presumably indicate coherent energy propagation.

Finally, higher-resolution studies of linewidths and spectral dynamics in relatively high-concen-

tration samples (preferably powders to eliminate radiative transfer) might reveal subtleties which were unobservable in our experiments. Increased resonance linewidths at higher concentration (both with and without application of a magnetic field) would possibly signify an excitonlike bandwidth, from which J could be roughly determined. With an order of magnitude higher than our present resolution, any changes in width of the narrowed components in time could also be easily detected.

Unraveling the details of the ruby spectrum has occupied numerous spectroscopists over many decades. During the last few years, this task has been considerably aided with the refinement of modern laser techniques. Yet, a complete understanding of this complex and elusive system must still await future experimental and theoretical effort.

Note added in proof. Recent numerical studies of dipole-dipole transfer on a face-centered-cubic

lattice have established that when $c < 0.2$, Eq. (8) with $f_n(t) = \cosh(W_{on}t)$ is a good approximation to $R(t)$ in the interval $1 \geq R(t) \geq 0.05$ [W. Y. Ching, D. L. Huber, and B. Barnett, *Phys. Rev. B* **17**, 5026 (1978)]. This result supports the fitting procedures outlined in Sec. IV B since our data are confined to the interval $1 \geq R(t) \geq 0.1$.

ACKNOWLEDGMENTS

A number of people have made valuable suggestions during the course of these experiments. In particular, we wish to acknowledge stimulating conversations with R. Orbach, G. F. Imbusch, and S. Geschwind, and the assistance of D. S. Hamilton in portions of this work. We also wish to thank Ken Sherwin at Stanford University for the loan of some ruby samples. This research was sponsored by grants from the NSF and the University of Wisconsin Research Council.

*Present address: Research Staff, Ford Motor Company, Dearborn, Mich. 48121.

†Permanent address: Soreq Nuclear Research Center, Yavne, Israel.

¹Edmond Becquerel, *La Lumiere—Ses Causes et Ses Effects* (Librairie de Firmin Didot Freres, Fils et Cie, Imprimeurs de L'Institute, Paris, 1867), Chap. IV.

²H. du Bois and G. J. Elias, *Ann. Phys. (Paris)* **27**, 233 (1908).

³See, e.g., O. Deutschbein, *Z. Phys.* **77**, 489 (1934); also A. L. Schawlow, D. L. Wood and A. M. Clogston, *Phys. Rev. Lett.* **3**, 271 (1959).

⁴See, e.g., S. Geschwind, G. E. Devlin, R. L. Cohen, and S. R. Chinn, *Phys. Rev.* **137**, 1087 (1965).

⁵G. F. Imbusch, *Phys. Rev.* **153**, 326 (1967).

⁶S. K. Lyo, *Phys. Rev. B* **3**, 3331 (1971).

⁷N. A. Kurnit, I. D. Abella, and S. R. Hartmann, *Phys. Rev. Lett.* **13**, 567 (1964).

⁸A. Szabo, *Phys. Rev. Lett.* **25**, 924 (1970).

⁹A. Szabo, *Phys. Rev. B* **11**, 4512 (1975).

¹⁰J. Koo, L. R. Walker, and S. Geschwind, *Phys. Rev. Lett.* **35**, 1669 (1975).

¹¹P. M. Selzer, D. S. Hamilton, and W. M. Yen, *Phys. Rev. Lett.* **38**, 853 (1977).

¹²P. M. Selzer and W. M. Yen, *Opt. Lett.* **1**, 90 (1977).

¹³R. Flach, D. S. Hamilton, P. M. Selzer, and W. M. Yen, *Phys. Rev. B* **15**, 1248 (1977).

¹⁴T. Kushida and E. Takushi, *Phys. Rev. B* **12**, 824 (1975).

¹⁵Since strong resonance fluorescence is observed, the excited level cannot relax rapidly to some lower state. Therefore, any phonon-induced relaxation will involve a higher level and should exhibit thermal activation.

¹⁶A. Compaan, *Phys. Rev. B* **5**, 4450 (1972).

¹⁷R. Orbach, in *Optical Properties of Ions in Crystals*, edited by H. M. Crosswhite and H. W. Moos (Inter-

science, New York, 1967), p. 445.

¹⁸R. J. Birgeneau, *J. Chem. Phys.* **50**, 4282 (1969).

¹⁹P. M. Selzer, D. A. Hamilton, R. Flach, and W. M. Yen, *J. Lumin.* **12/13**, 737 (1976).

²⁰D. S. Hamilton, P. M. Selzer, and W. M. Yen, *Phys. Rev. B* **16**, 1858 (1977).

²¹T. Holstein, S. K. Lyo, and R. Orbach, *Phys. Rev. Lett.* **36**, 891 (1976).

²²See, e.g., B. Di Bartolo, *Optical Interactions in Solids* (Wiley, New York, 1968), p. 343.

²³M. Blume, R. Orbach, A. Kiel, and S. Geschwind, *Phys. Rev.* **139**, 314 (1965).

²⁴J. E. Rives and R. S. Meltzer, *Phys. Rev. B* **16**, 1808 (1977).

²⁵A. L. Schawlow, in *Advance in Quantum Electronics*, edited by J. R. Singer (Columbia U. P., New York, 1961), p. 59.

²⁶H. B. Huntington, in *Advances in Solid State Physics*, edited by F. Seitz and D. Turnbull (Academic, New York, 1956), Vol. VII, p. 213.

²⁷A. A. Kaplyanskii and A. K. Przkeviskii, *Sov. Phys.—Solid State* **9**, 190 (1967); L. F. Mollenauer and A. L. Schawlow, *Phys. Rev.* **168**, 309 (1968).

²⁸R. Orbach (private communication).

²⁹T. Holstein, S. K. Lyo, and R. Orbach, *Phys. Rev. B* **15**, 4693 (1977).

³⁰D. L. Huber, D. S. Hamilton, and B. Barnett, *Phys. Rev. B* **16**, 4642 (1977).

³¹The right-hand side of Eq. (10) differs by a factor of $2^{3/s-1}$ from an expression derived by M. Inokuti and F. Hirayama [*J. Chem. Phys.* **43**, 1978 (1965)]. Their approach omits back-transfer and is equivalent to taking $f_n(t) = 1$.

³²It should be emphasized that W_0 is only a nominal nearest-neighbor transfer rate. Near-neighbor pairs in ruby are strongly coupled by the exchange interaction and hence are regarded as two-ion systems. The pro-

- per interpretation of W_0 is that it is a parameter characterizing the transfer between ions separated by approximately the average spacing.
- ³³T. Holstein, S. K. Lyo, and R. Orbach, *Phys. Rev. B* 16, 934 (1977).
- ³⁴J. C. Murphy, L. C. Aamodt, and C. K. Jen, *Phys. Rev. B* 9, 2009 (1974).
- ³⁵I. Ya. Gerlovin, *Sov. Phys.-Solid State* 16, 397 (1974).
- ³⁶J. Heber, *Phys. Status Solidi* 42, 497 (1970).
- ³⁷J. Heber and H. Murmann, *Z. Phys. B* 26, 145 (1977); also J. Heber and H. Murmann, *J. Lumin.* 12/13, 769 (1976).
- ³⁸Scattered laser light became a problem at shorter delays. However, lifetimes of R_1 were also taken with the laser exciting R_2 in order to reduce the scattered light. This allowed measurements in as close as 50 μ sec, with still no deviation from exponential decay.
- ³⁹P. Kisliuk, N. C. Chang, P. L. Scott, and M. H. L. Pryce, *Phys. Rev.* 184, 367 (1969).
- ⁴⁰J. Heber and H. Murmann, *Z. Phys. B* 26, 137 (1977).
- ⁴¹F. Keffer and T. Oguchi, *Phys. Rev.* 115, 1428 (1959).
- ⁴²P. W. Anderson, *Phys. Rev.* 109, 1492 (1958).
- ⁴³This is strictly true only as long as the ion-lattice interaction time is much longer than the nearest-neighbor interaction time $\sim \hbar/J$. At a high enough temperature, ion-lattice interactions will disrupt the coherence, and conduction will be reduced.
- ⁴⁴D. R. Mason and J. S. Thorp, *Proc. Phys. Soc. Lond.* 87, 49 (1966); C. A. Bates and R. F. Jasper, *J. Phys. C* 4, 2341 (1971).
- ⁴⁵Residual temperature-dependent radiative trapping and changes in linewidth and line position with temperature make reliable quantitative temperature-dependent measurements difficult to obtain.
- ⁴⁶The possible influence of clustering could be investigated by a detailed study of lifetimes as a function of laser position. Our efforts in this regard have so far been frustrated by residual radiative trapping, even in finely ground powders.
- ⁴⁷A. Z. Genack, R. M. Macfarlane, and R. G. Brewer, *Phys. Rev. Lett.* 37, 1078 (1976).
- ⁴⁸P. F. Liao and S. R. Hartmann, *Opt. Commun.* 8, 310 (1973); also A. Szabo and M. Kroll, *Opt. Lett.* 2, 10 (1978).